

# Spectral and Energy Efficiency of DCO-OFDM in Visible Light Communication Systems with Finite-Alphabet Inputs

Ruixin Yang, Shuai Ma, Zihan Xu, Hang Li, Xiaodong Liu, Xintong Ling, Xiong Deng, Xun Zhang, Shiyin Li

**Abstract**—The bound of the information transmission rate of direct current biased optical orthogonal frequency division multiplexing (DCO-OFDM) for visible light communication (VLC) with finite-alphabet inputs is yet unknown, where the corresponding spectral efficiency (SE) and energy efficiency (EE) stems out as the open research problems. In this paper, we derive the exact achievable rate of the DCO-OFDM system with finite-alphabet inputs for the first time. Furthermore, we investigate SE maximization problems of the DCO-OFDM system subject to both electrical and optical power constraints. By exploiting the relationship between the mutual information and the minimum mean-squared error, we propose a multi-level mercury-water-filling power allocation scheme to achieve the maximum SE. Moreover, the EE maximization problems of the DCO-OFDM system are studied, and the Dinkelbach-type power allocation scheme is developed for the maximum EE. Numerical results verify the effectiveness of the proposed theories and power allocation schemes.

**Index Terms**—Visible light communications, DCO-OFDM, finite-alphabet input, spectral efficiency, energy efficiency.

## I. INTRODUCTION

### A. Motivation and Contributions

As the number of Internet of Things (IoT) devices increases tremendously, the radio frequency (RF) wireless networks are facing an ever-growing bandwidth burden to support huge and high-speed data transfer [1]–[3]. It is reported that more than 80% of wireless data is generated in the indoor environment [4], [5]. As a result, visible light communication (VLC) [6] has emerged as a promising technology to provide high-speed data transmission and illumination service simultaneously due to the huge unlicensed visible light spectrum for future IoT applications [7], [8]. By using the ordinary light emitting

diodes (LEDs) at the transmitter side and the simple intensity modulation and direct detection (IM/DD) at the receiver side, VLC can simultaneously support high-speed communication and illumination without electromagnetic interference to the conventional RF networks [9]–[12].

From the wireless communication point of view, the VLC system, similar to the RF system, still faces the issue of inter-symbol interference (ISI) resulting from limited modulation bandwidth of LEDs [13] and multipath distortion [14]. Thus, the orthogonal frequency division multiplexing (OFDM) based techniques are introduced into the VLC system against the ISI and enhance the communication capacity. There are two typical OFDM-based transmission schemes: direct current (DC) biased optical OFDM (DCO-OFDM) and asymmetrically clipped optical OFDM (ACO-OFDM). Specifically, to guarantee that the transmitted signals are positive, DCO-OFDM adds a DC-bias to the time-domain signals and clips the remaining negative signals to zero, while ACO-OFDM only transmits the positive parts of the OFDM waveform. Note that if the DC-bias power is neglected, DCO-OFDM can achieve the Shannon capacity while ACO-OFDM has a 3-dB penalty [15]. In practice, the DCO-OFDM system usually operates with finite-alphabet inputs such as pulse amplitude modulation (PAM) and quadrature amplitude modulation (QAM).

Most of the existing literature on the DCO-OFDM system adopted the assumption that if the number of subcarriers is large, the time domain signal after the inverse fast Fourier transform (IFFT) is approximately Gaussian distributed [16]–[19]. However, according to the central limit theorem, only if the number of subcarriers tends to infinity, and the frequency domain symbols are independent, the time domain signal equivalently follows the Gaussian distribution, whatever the alphabet set is a continuous set or a finite constellation set. Therefore, some approximation errors exist to some extent. Meanwhile, when the random process is unbounded, the clipping operator cannot be avoided, and the clipping noise may cause the inevitable information loss [18], [20]. Under such an assumption, existing models cannot accurately depict the achievable rate of the DCO-OFDM system with finite-alphabet inputs, and the corresponding bound of the information transmission rate is yet unknown. Thus, the spectrum efficiency (SE) and energy efficiency (EE) of the DCO-OFDM system still need further investigation.

Besides, unlike the conventional RF communication sys-

R. Yang, S. Ma and S. Li are with the School of Information and Control Engineering, China University of Mining and Technology, Xuzhou, 221116, China. (e-mail: {ray.young, mashuai001, lishiyin}@cumt.edu.cn).

Z. Xu is with Spreadtrum Communications (Shanghai) Co., Ltd., Shanghai 201203, China (e-mail: zihan.xu@unisoc.com).

H. Li is with the Shenzhen Research Institute of Big Data, Shenzhen 518172, Guangdong, China. (email: hangdavidli@163.com).

X. Liu is with the School of Information Engineering, Nanchang University, Nanchang 330031, China (e-mail: xiaodongliu@ieec.org).

X. Ling is with the National Mobile Communications Research Laboratory, Southeast University, and the Purple Mountain Laboratories, Nanjing, China. (e-mail: xtling@seu.edu.cn).

X. Deng is with the Center for Information Photonics and Communications, Southwest Jiaotong University, Chengdu 610031, China.(email: xiongdeng@swjtu.edu.cn).

X. Zhang is with Institut Suprieur dElectronique de Paris, ISEP Paris, France. (e-mail: xun.zhang@isep.fr).

tems, where only the electrical power constraint is considered in most scenarios, the average optical power constraint plays an important role in the illumination requirement [9], [11] and should also be considered in the discussions of SE and EE.

With the aforementioned issues, in this paper, we consider such a typical DCO-OFDM-based VLC system and investigate the optimal power allocation over subcarriers to maximize the SE and EE. Our main contributions of this paper are summarized as follows:

- To our best knowledge, the theoretical bound of the information transmission rate of the DCO-OFDM system with finite-alphabet inputs remains unknown. In this work, we derive the information rate of the DCO-OFDM system with finite-alphabet inputs for the first time. Specifically, we derive the exact achievable rate expression of the DCO-OFDM system without the information loss. Moreover, we derive the closed-form lower bound for the derived achievable rate. The obtained expressions can be used as the performance metrics, and we also apply them in the transmission design.
- Based on the closed-form lower bound of the achievable rate, we jointly optimize DC-bias, and power allocation of subcarriers to maximize the SE of the DCO-OFDM system under both average optical power and total electrical transmitted power constraints. We find that the optimal DC-bias without information loss can be presented in a closed-form expression. Then, by restricting both optical and electrical power constraints, the optimal power allocation can be obtained by employing the interior-point algorithm.
- Next, we further study the SE maximization problem based on the exact achievable rate expression under the same constraints above. By exploiting the Karush-Kuhn-Tucker (KKT) conditions and the relationship between the mutual information and the minimum mean-squared error (MMSE)<sup>1</sup> [21], we propose a multi-level mercury-water-filling power allocation scheme to achieve the maximum of SE [22], [23]. It is shown that the power allocation behaves differently with respect to the channel gain in the low and high power domains.
- Finally, we investigate the power allocation to maximize the EE of the DCO-OFDM system derived two achievable rate metrics, respectively. We employ the Dinkelbach-type algorithm to convert the concave-linear fractional problem into a sequence of convex sub-problems, and then obtain the optimal power allocation by the interior-point algorithm. In addition, we reveal that the optimal power allocation of the EE maximization problem with finite-alphabet inputs is related to the SE requirement. For the low SE requirement, the allocated power of each subcarrier is proportional to the channel gain. While for the high SE requirement, the allocated power of each subcarrier is inversely proportional to the channel gain.

## B. Related Works and Organization

Most of the existing literature on SE and EE of the DCO-OFDM system study that the time domain signal output by IFFT is approximately Gaussian distributed when the number of subcarriers is large [16]–[19], which causes signal approximation errors, as well as clipping noise and information loss with the clipping process [18], [20].

It should be pointed out that the SE of the DCO-OFDM system has been extensively studied for different input constraints. For example, under the optical power constraint and a target bit error rate (BER), the adaptive modulation scheme was employed in [16] to maximize the SE, and it was shown that the SE of ACO-OFDM is higher than that of DCO-OFDM in the low-SNR region while it has a 50% reduction compared to DCO-OFDM at high-SNR region. For uniform power within an optimized band, the authors in [24] proposed a discrete bit loading algorithm to maximize the achievable rate of the DCO-OFDM system. For the single-LED case, the signal-to-noise-plus-distortion ratio (SNDR) of DCO-OFDM was maximized by jointly optimizing both the DC-bias and the information-carrying power under both the optical and electrical power constraints [18]. In the case with multiple LEDs, the SNDR maximization problem in the DCO-OFDM system was studied in [19] by properly designing the biased beamforming with the optical power constraint. By utilizing generalized mutual information, the lower bound of information rate was derived in [25] for the DCO-OFDM system under the average optical power constraint.

Recently, due to the increasing number of IoT devices, the research on EE has attracted great attention to reduce consumption and prolong the lifetime [26]–[28]. It was reported in [17] that both the energy and spectrum efficiency achieved with DCO-OFDM is higher than that obtained by ACO-OFDM in the case that a constant DC-bias power is given for the illumination requirement. By replacing the negative parts of signals with their absolute values, a power-efficient symbol recovery scheme for the DCO-OFDM system was proposed in [29], which can improve the symbol error rate (SER) performance for a given DC-bias. Under the constraints of the BER and the total transmitted power, the authors in [30] investigated the achievable rate maximization problem for the DCO-OFDM system, and further optimized transmitted power to achieve the tradeoff between SE and EE.

It was reported in [31] that the mutual information maximizing design and classic power allocation scheme based on Gaussian distributed assumption will lead to a significant loss. However, to the best of our knowledge, only a few works have investigated the SE and EE of the DCO-OFDM with finite-alphabet inputs. The most relevant work is [32], where the EE maximization problem of DCO-OFDM was studied by designing the optimal solution of the modulation order and power allocation under the minimum SE requirement and a total transmitted power constraint. However, since the mutual information does not have the closed-form expression, the authors in [32] adopted the closed-form lower bound and upper bound to approximate the exact mutual information to solve the optimal power allocation problem. In our study, we exploit

<sup>1</sup>  $\frac{\partial}{\partial \text{SNR}} I(\text{SNR}) = \text{MMSE}(\text{SNR})$ , where SNR denotes signal-to-noise ratio.

the relationship between the mutual information and MMSE to deal with the non-closed-form expression. Moreover, we study the bound of the information transmission rate of the DCO-OFDM system based on finite-alphabet inputs and the optimal DC-bias such that the clipping can be avoided, which is different from [18] and [19] with clipping noise, and propose the optimal power allocation scheme to maximize SE and EE of the DCO-OFDM system under the constraints of average optical power and total electrical transmitted power, and further consider the minimum SE requirement when maximizing EE.

The rest of this paper is organized as follows. The system model of the considered DCO-OFDM system is presented in Section II. The achievable rate expressions of DCO-OFDM are derived in Section III. The SE and EE maximization problems of the DCO-OFDM system are respectively studied in Section IV and Section V. The simulation results are presented in Section VI. Finally, the conclusions are drawn in Section VII.

*Notations:* Expected value of a random variable  $z$  is denoted by  $\mathbb{E}\{z\}$ .  $(\cdot)^*$  represents conjugate transformation.  $[x]^+$  denotes  $\max\{x, 0\}$ .  $\text{Re}(\cdot)$  and  $\text{Im}(\cdot)$  denote the real and imaginary parts of their argument, respectively.  $\partial f(\cdot)/\partial x$  represents the partial derivative of function  $f(\cdot)$ . Given a variable  $y$ ,  $\mathbb{E}\{z|y\}$  represents the conditional expectation of  $z$  for given  $y$ .  $I(X; Y)$  represents the mutual information of  $X$  and  $Y$ .

## II. SYSTEM MODEL

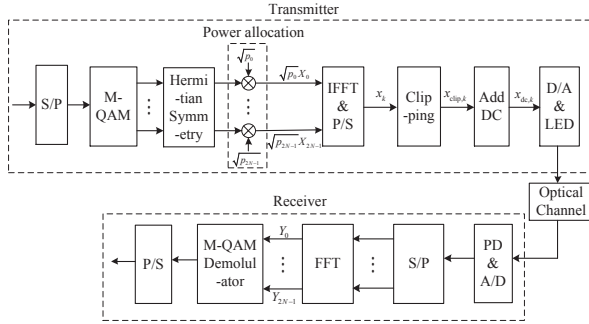


Fig. 1: The schematic diagram of a DCO-OFDM VLC system.

In this paper, we consider both the SE and EE optimization problems for the DCO-OFDM system with finite-alphabet inputs shown in Fig. 1. At the transmitter side, the input bit streams are modulated by an  $M$ -ary QAM after serial-to-parallel (S/P) conversion. Due to the IM/DD, the transmit signal is required not only to be non-negative but also to be real-valued. In order to ensure that the output signal of the IFFT is a real-valued VLC signal, the IFFT input symbols of  $2N$  subcarriers after Hermitian symmetry should satisfy

$$\sqrt{p_{2N-i}}X_{2N-i} = \sqrt{p_i}X_i^*, \quad i = 1, \dots, N-1, \quad (1)$$

where  $X_i$  is the signal of the  $i$ th subcarrier, which should be  $X_0 = X_N = 0$  to block the DC component. Without loss of generality, we can assume  $\mathbb{E}\{|X_i|^2\} = 1$ . Besides, let  $p_i$  denote the allocated power for the  $i$ th subcarrier, and follow

$p_0 = p_N = 0$ , and  $p_{2N-i} = p_i, i = 1, \dots, N-1$ . Then, the IFFT output signal  $x_k$  in the time domain is given by

$$x_k = \frac{1}{\sqrt{2N}} \sum_{i=0}^{2N-1} \sqrt{p_i} X_i \exp\left(j \frac{\pi k i}{N}\right) \quad (2a)$$

$$= \frac{1}{\sqrt{2N}} \left( \sum_{i=1}^{N-1} \sqrt{p_i} X_i \exp\left(j \frac{\pi k i}{N}\right) + \sum_{i=1}^{N-1} \left( \sqrt{p_i} X_i \exp\left(j \frac{\pi k i}{N}\right) \right)^* \right) \quad (2b)$$

$$= \sqrt{\frac{2}{N}} \sum_{i=1}^{N-1} \sqrt{p_i} \text{Re} \left( X_i \exp\left(j \frac{\pi k i}{N}\right) \right), \quad (2c)$$

where  $k = 0, \dots, 2N-1$ . It is easy to find that  $\mathbb{E}\{x_k\} = 0$ .

To guarantee the VLC signal non-negative, the clipping operator is applied. Specifically, the time domain signal  $x_k$  is converted to clipped signal  $x_{\text{clip},k}$  by clipping at the level of  $-I_{\text{dc}}$ , where  $I_{\text{dc}}$  is the DC-bias and the clipping operator is defined as

$$x_{\text{clip},k} = \begin{cases} x_k & x_k \geq -I_{\text{dc}}, \\ -I_{\text{dc}} & x_k \leq -I_{\text{dc}}. \end{cases} \quad (3)$$

Then  $x_{\text{clip},k}$  is added with  $I_{\text{dc}}$  which only affects the 0th subcarrier in the frequency domain. Thus, we obtain the non-negative signal

$$x_{\text{dc},k} = x_{\text{clip},k} + I_{\text{dc}}. \quad (4)$$

If we want to avoid the information loss brought by the clipping noise, a feasible way is to avoid the clipping operation, i.e., the amplitude of the time domain signal  $x_k$  should be bounded, and an appropriate DC-bias  $I_{\text{dc}}$  should satisfy

$$x_k + I_{\text{dc}} \geq \min\{x_k\} + I_{\text{dc}} \geq 0. \quad (5)$$

Moreover, the digital signal  $x_{\text{dc},k}$  is converted to the analog signal via digital-to-analog convertor (DAC) and then transmitted by LED. To satisfy the illumination and human eye safety requirements, the average optical power is restricted, i.e.,

$$\mathbb{E}\{x_{\text{dc},k}\} \leq P_o, \quad (6)$$

where  $P_o$  represents the maximum average optical power budget.

Besides, for the practical electrical circuits consideration, the total electrical transmitted power of the VLC system should also be constrained, i.e.,

$$\sum_{k=0}^{2N-1} \mathbb{E}\{x_{\text{dc},k}^2\} \leq P_e. \quad (7)$$

where  $P_e$  is the maximum total electrical transmitted power budget.

Note that the channel of the VLC system is generally low-pass [18], [33], and the channel gain difference between each subcarrier can be utilized via allocating proper power to each subcarrier to improve the performance of the VLC system. Indoor VLC channel includes two components: the line-of-sight (LOS) link between the transmitter and the receiver;

and the diffuse link that is the superposition of all non-LOS components caused by one or more reflections on the surface of the room.

Let  $H_{L,i} = \eta_L e^{-j2\pi f_i \tau_L}$  denote the channel gain of the LOS link of the  $i$ th subcarrier, where  $\eta_L$  is the generalized Lambertian radiator [8], [33] expressed as

$$\eta_L = \frac{(m+1) A_r \cos(\varphi)}{2\pi d^2} \cos^m(\theta) T(\varphi) G(\varphi) \text{rect}(\varphi/\Psi). \quad (8)$$

In (8),  $m = -\ln 2 / \ln(\cos \Phi_{1/2})$  denotes the order of Lambertian emission, and  $\Phi_{1/2}$  is the semi-angle at half power.  $A_r$  denotes the effective detector area of the photodetector (PD),  $\varphi$  and  $\theta$  are the incidence and irradiance angles from the LED to the PD, respectively,  $T(\varphi)$  and  $G(\varphi)$  are the optical filter gain and the concentrator gain of the receiver, respectively,  $\Psi$  represents the field-of-view (FOV) of the receiver, the rectangular function  $\text{rect}(x)$  takes 1 whenever  $|x| \leq 1$ , and is 0 otherwise,  $f_i$  denotes the frequency of the  $i$ th subcarrier,  $\tau_L = d/c$  is the signal propagation delay of the LOS link between the LED to the PD,  $d$  is the distance between the LED to the PD, and  $c$  stands for the speed of light.

Let  $H_{D,i} = \frac{\eta_D}{1+j2\pi\tau_D f_i}$  denote the channel gain of the diffuse link of the  $i$ th subcarrier [34], where  $\eta_D = \frac{A_r}{A_{\text{room}}} \frac{\rho}{1-\rho}$  is the diffuse channel gain factor. Here,  $A_{\text{room}}$  is the surface of the room and  $\rho$  is the average value of the room reflectivity factor. Moreover,  $\tau_D = -\frac{1}{\ln \rho} \frac{4V_{\text{room}}}{A_{\text{room}} c}$  is the time constant, and  $V_{\text{room}}$  is the volume of the room. Then, the total channel gain  $H_i$  of the  $i$ th subcarrier can be expressed as

$$H_i = H_{L,i} + H_{D,i}, \quad i = 0, \dots, 2N-1. \quad (9)$$

At the receiver, the received optical signal is converted to analog electrical signal by the PD. Then, the digital signal is obtained by an analog-to-digital convertor (ADC). Finally, the bit stream is recovered through the fast Fourier transform (FFT) and demodulation operations.

Specifically, the frequency domain expression of the received signal  $Y_i$  can be written as

$$Y_i = H_i \sqrt{p_i} X_i + Z_i, \quad i = 1, \dots, N-1, \quad (10)$$

where  $Y_i$  and  $H_i$  represent the received signal and the total channel gain at the  $i$ th subcarrier, respectively.  $Z_i$  is the additive white Gaussian noise (AWGN) with zero-mean, i.e.,  $Z_i \sim \mathcal{CN}(0, \sigma^2 W)$ , where  $\sigma^2$  represents the noise power spectral density (PSD), and the bandwidth of each subcarrier is  $W$ .

### III. ACHIEVABLE RATE OF THE DCO-OFDM SYSTEM

Recall that in most existing works, the achievable rates of the DCO-OFDM system are derived based on the assumption that the time domain signal obtained after the IFFT is approximately Gaussian distributed, and the exact achievable

rate without the information loss of the DCO-OFDM system with finite-alphabet inputs is still unknown.

Here, we consider a system that the discrete constellation points are equiprobably drawn from discrete constellations set  $\{X_{i,k}\}_{k=1}^M$  with cardinality  $M$ , where  $X_{i,k}$  is the  $k$ th constellation point of the  $i$ th subcarrier. Thus, the achievable rate  $R_{F,i}(p_i)$  of the  $i$ th subcarrier can be expressed as

$$R_{F,i}(p_i) = I_i(X_i; Y_i) \quad (11a)$$

$$= W \left( \log_2 M - \frac{1}{\ln 2} \right) - \sum_{n=1}^M \frac{W}{M} \mathbb{E}_{Z_i} \left\{ \log_2 \sum_{k=1}^M \exp(-d_{n,k}) \right\}, \quad (11b)$$

where  $d_{n,k} \triangleq \frac{|H_i \sqrt{p_i} (X_{i,n} - X_{i,k}) + Z_i|^2}{\sigma^2 W}$  is a measure of the difference between discrete constellation points  $X_{i,n}$  and  $X_{i,k}$ , and  $\mathbb{E}_{Z_i} \{\cdot\}$  is the expectation of the noise  $Z_i$ . The detailed derivation of (11b) is given in Appendix A. Moreover, it is easy to find that  $R_{F,i}(p_i)$  is a concave function with respect to the power allocation  $p_i$  [31], [35]. Thus, the total achievable rate of the DCO-OFDM system with finite-alphabet inputs is given by

$$R_{F,\text{total}}(\{p_i\}) = \sum_{i=1}^{N-1} R_{F,i}(p_i). \quad (12)$$

Note that, for  $M \geq 2$ , the expectation term in the achievable rate (11b) is a non-integrable function and lacks of closed-form expression, making it challenging for resource allocation. To address this challenge, we further derive the lower bound of (11b) with closed-form expression. Since  $\log_2(\cdot)$  is a concave function, the upper bound of the expectation term in (11b) is given by

$$\mathbb{E}_{Z_i} \left\{ \log_2 \sum_{k=1}^M \exp(-d_{n,k}) \right\} \leq \log_2 \sum_{k=1}^M \mathbb{E}_{Z_i} \{ \exp(-d_{n,k}) \} \quad (13a)$$

$$= \log_2 \sum_{k=1}^M \int_{Z_i} \exp(-d_{n,k}) \frac{1}{\pi \sigma^2 W} \exp\left(-\frac{|Z_i|^2}{\sigma^2 W}\right) dZ_i \quad (13b)$$

$$= -1 + \log_2 \sum_{k=1}^M \exp\left(-\frac{p_i |H_i|^2 |X_{i,k} - X_{i,m}|^2}{2\sigma^2 W}\right), \quad (13c)$$

where (13a) is due to the Jensen's inequality [36].

Thus, let  $R_{L,i}(p_i)$  represent the lower bound of mutual information of the  $i$ th subcarrier with finite-alphabet inputs and is given by (14).

Similar to  $R_{F,i}(p_i)$ ,  $R_{L,i}(p_i)$  is also a concave function with respect to the power allocation  $p_i$ . The corresponding lower bound of total achievable rate of the DCO-OFDM

$$R_{L,i}(p_i) = W \left( \log_2 M + 1 - \frac{1}{\ln 2} \right) - \sum_{n=1}^M \frac{W}{M} \log_2 \sum_{k=1}^M \exp\left(-\frac{p_i |H_i|^2 |X_{i,n} - X_{i,k}|^2}{2\sigma^2 W}\right). \quad (14)$$

system is given by

$$R_{L,\text{total}}(\{p_i\}) = \sum_{i=1}^{N-1} R_{L,i}(p_i). \quad (15)$$

As same as [36], there is a constant gap  $C \triangleq \frac{1}{\ln 2} - 1$  between  $R_F(p_i)$  and  $R_L(p_i)$  when  $p_i \rightarrow \infty$  or  $p_i \rightarrow 0$ , and  $R_A(p_i) \triangleq R_L(p_i) + C$  can also be as a low-complexity approximation of  $R_F(p_i)$ , which always converges to  $R_F(p_i)$  with  $p_i \rightarrow \infty$  or  $p_i \rightarrow 0$ , while exceeds  $R_F(p_i)$  in the medium region. Then, the corresponding total achievable rate is given by  $R_{A,\text{total}}(\{p_i\}) = \sum_{i=1}^{N-1} R_{A,i}(p_i)$ , which is still concave with respect to the power allocation  $p_i$ .

#### IV. SPECTRAL EFFICIENCY MAXIMIZATION OF THE DCO-OFDM SYSTEM

In this section, we investigate the SE maximization problem of the DCO-OFDM system subject to the maximum average optical power and the maximum total electrical transmitted power constraints. Specifically, we start from a simple case of  $R_{L,\text{total}}(\{p_i\})$  in (15) with the closed-form expression and then the more challenging case of  $R_{F,\text{total}}(\{p_i\})$  in (12) without a closed-form expression.

##### A. SE Maximization based on $R_{L,\text{total}}(\{p_i\})$

With the closed-form expression of lower bound of the achievable rate (15), the SE can be expressed as

$$\text{SE}_L(\{p_i\}) = \frac{R_{L,\text{total}}(\{p_i\})}{2NW}. \quad (16)$$

Then, we aim to maximize the SE of the DCO-OFDM system under amplitude constraint, average optical power constraint and total electrical transmitted power constraint, which can be mathematically formulated as

$$\underset{\{p_i\}, I_{\text{dc}}}{\text{maximize}} \quad \text{SE}_L(\{p_i\}) \quad (17a)$$

$$\text{s.t.} \quad x_k + I_{\text{dc}} \geq 0, \quad (17b)$$

$$\mathbb{E}\{x_{\text{dc},k}\} \leq P_o, \quad (17c)$$

$$\sum_{k=0}^{2N-1} \mathbb{E}\{x_{\text{dc},k}^2\} \leq P_e, \quad (17d)$$

$$p_i \geq 0, \quad i = 1, \dots, N-1. \quad (17e)$$

Although the joint design of variables DC-bias  $I_{\text{dc}}$  and power allocation  $p_i$  complicates the optimization problem, it can be seen from problem (17) that the objective function is only related to the power allocation  $p_i$ , and it is monotonically increasing as  $p_i$  increases. Moreover, based on (4) and (17b), the total electrical transmitted power in (17d) can be expressed as

$$\sum_{k=0}^{2N-1} \mathbb{E}\{x_{\text{dc},k}^2\} = \sum_{k=0}^{2N-1} \mathbb{E}\{x_k^2\} + \sum_{k=0}^{2N-1} \mathbb{E}\{I_{\text{dc}}^2\} \quad (18a)$$

$$= 2 \sum_{i=1}^{N-1} p_i + 2N \mathbb{E}\{I_{\text{dc}}^2\}, \quad (18b)$$

where (18a) is true since the time domain signal  $x_k$  is not clipped, i.e.,  $x_{\text{clip},k} = x_k$ , (18b) follows from the Parseval's theorem, and the total electrical transmitted power of time domain signal  $x_k$  is  $\sum_{k=0}^{2N-1} \mathbb{E}\{x_k^2\} = \sum_{i=0}^{2N-1} p_i = 2 \sum_{i=1}^{N-1} p_i$ . Thus, combining with the total electrical transmitted power constraint, we find that more power should be allocated for the information-carrying  $p_i$  and less power should be allocated for the DC-bias  $I_{\text{dc}}$  to maximize the achievable rate  $R_{L,\text{total}}(\{p_i\})$ . Specifically, the optimal value of  $I_{\text{dc}}^{\text{opt}}$  should be the minimum DC-bias without clipping the signal  $x_k$ .

Furthermore, from (2c), we have

$$x_k \geq -\sqrt{\frac{2}{N}} \sum_{i=1}^{N-1} \sqrt{p_i} |X_i|. \quad (19)$$

Then,  $I_{\text{dc}}^{\text{non-clipping}}$  which minimizes the power of the DC-bias without clipping the signal  $x_k$  can be written as

$$I_{\text{dc}}^{\text{non-clipping}} = \sqrt{\frac{2}{N}} \sum_{i=1}^{N-1} \sqrt{p_i} |X_i|. \quad (20)$$

As a result, combining (4), (17b) and (20), the average optical power can be rewritten as

$$\mathbb{E}\{x_{\text{dc},k}\} = \mathbb{E}\{x_{\text{clip},k} + I_{\text{dc}}^{\text{non-clipping}}\} \quad (21a)$$

$$= \mathbb{E}\{x_k\} + \mathbb{E}\{I_{\text{dc}}^{\text{non-clipping}}\} \quad (21b)$$

$$= \sqrt{\frac{2}{N}} \sum_{i=1}^{N-1} \sqrt{p_i} \mathbb{E}\{|X_i|\}. \quad (21c)$$

According to Cauchy-Schwarz inequality

$$\left(\sum_{i=1}^n a_i\right)^2 \leq n \sum_{i=1}^n a_i^2, \quad a_i \geq 0, \quad (22)$$

the upper bound of the square of the average optical power is given by

$$\left(\sqrt{\frac{2}{N}} \sum_{i=1}^{N-1} \sqrt{p_i} \mathbb{E}\{|X_i|\}\right)^2 \leq \frac{2(N-1)}{N} \sum_{i=1}^{N-1} p_i \mathbb{E}^2\{|X_i|\}. \quad (23)$$

Thus, the average optical power constraint (17c) can be restricted to

$$\sum_{i=1}^{N-1} p_i \mathbb{E}^2\{|X_i|\} \leq \frac{NP_o^2}{2(N-1)}. \quad (24)$$

Meanwhile, by substituting  $I_{\text{dc}}^{\text{non-clipping}}$  in (20) into (18b), the total electrical transmitted power can be written as

$$\sum_{k=0}^{2N-1} \mathbb{E}\{x_{\text{dc},k}^2\} = 2 \sum_{i=1}^{N-1} p_i + 4 \mathbb{E}\left\{\left(\sum_{i=1}^{N-1} \sqrt{p_i} |X_i|\right)^2\right\}. \quad (25)$$

Applying the inequality (22), the upper bound of the total

electrical transmitted power (25) is given as

$$\sum_{k=0}^{2N-1} \mathbb{E} \{x_{\text{dc},k}^2\} \leq 2 \sum_{i=1}^{N-1} p_i + 4 \mathbb{E} \left\{ (N-1) \sum_{i=1}^{N-1} p_i |X_i|^2 \right\}. \quad (26)$$

Thus, the constraint (17d) can be reformulated as

$$\sum_{i=1}^{N-1} p_i \leq \frac{P_e}{4N-2}. \quad (27)$$

Therefore, the SE maximization problem (17) can be transformed into

$$\underset{\{p_i\}}{\text{maximize}} \quad \text{SE}_L(\{p_i\}) \quad (28a)$$

$$\text{s.t.} \quad \sum_{i=1}^{N-1} p_i \mathbb{E}^2 \{|X_i|\} \leq \frac{NP_o^2}{2(N-1)}, \quad (28b)$$

$$\sum_{i=1}^{N-1} p_i \leq \frac{P_e}{4N-2}, \quad (28c)$$

$$p_i \geq 0, \quad i = 1, \dots, N-1. \quad (28d)$$

Note that the optimization problem (28) has a strictly concave objective function over its input power  $p_i$  and linear constraints, and thus can be efficiently solved by the interior-point algorithm. Such as the barrier method, it transforms the convex optimization problems into a sequence of equality constrained problems and applies Newton's method to them, or such as the primal-dual interior-point method, it modifies the corresponding KKT conditions and solves them by Newton's method [37], [38]. Besides, It has been implemented by standard convex optimization solvers such as CVX [39].

Besides, the SE based on  $R_{L,\text{total}}(\{p_i\})$  is denoted as  $\text{SE}_A$ , and the corresponding SE maximization power allocation problem is equivalent to the problem (17) without the optimality loss, which can be solved by the similar technique.

### B. SE Maximization based on $R_{F,\text{total}}(\{p_i\})$

In this subsection, we investigate the SE maximization problem of the DCO-OFDM system based on the exact mutual information (12). The SE achieved with exact mutual information is given by

$$\text{SE}_F(\{p_i\}) = \frac{R_{F,\text{total}}(\{p_i\})}{2NW}. \quad (29)$$

Similarly, the value of the DC-bias  $I_{\text{dc}}$  is the same as (20) to ensure that the transmitted DC-bias power is minimized while the signal  $x_k$  is not clipped. Thus, by considering the same constraints in problem (28), the SE maximization problem with finite-alphabet inputs can be reformulated as

$$\underset{\{p_i\}}{\text{maximize}} \quad \text{SE}_F(\{p_i\}) \quad (30)$$

$$\text{s.t.} \quad (28b), (28c), (28d).$$

Note that the objective function (30) is concave over  $p_i$ , and constraints (28b) and (28c) are affine functions over  $p_i$ . This type of optimization problem can be efficiently solved

based on the KKT conditions. To this end, we first derive the Lagrangian function of problem (30), which is given by

$$\mathcal{L}_F = - \sum_{i=1}^{N-1} R_{F,i}(p_i) + \lambda_1 \left( \sum_{i=1}^{N-1} p_i \mathbb{E}^2 \{|X_i|\} - \frac{NP_o^2}{2(N-1)} \right) + \lambda_2 \left( \sum_{i=1}^{N-1} p_i - \frac{P_e}{4N-2} \right), \quad (31)$$

where  $\lambda_1 \geq 0$ ,  $\lambda_2 \geq 0$  are the Lagrange multipliers corresponding to constraint (28b) and (28c) respectively. Then, the KKT conditions of problem (30) are given as

$$\frac{\partial \mathcal{L}_F}{\partial p_i} = - \frac{\partial R_{F,i}(p_i)}{\partial p_i} + \lambda_1 \mathbb{E}^2 \{|X_i|\} + \lambda_2 = 0, \quad (32a)$$

$$\lambda_1 \left( \sum_{i=1}^{N-1} p_i \mathbb{E}^2 \{|X_i|\} - \frac{NP_o^2}{2(N-1)} \right) = 0, \quad (32b)$$

$$\lambda_2 \left( \sum_{i=1}^{N-1} p_i - \frac{P_e}{4N-2} \right) = 0, \quad (32c)$$

$$\sum_{i=1}^{N-1} p_i \mathbb{E}^2 \{|X_i|\} - \frac{NP_o^2}{2(N-1)} \leq 0, \quad (32d)$$

$$\sum_{i=1}^{N-1} p_i - \frac{P_e}{4N-2} \leq 0, \quad (32e)$$

$$\lambda_1 \geq 0, \quad \lambda_2 \geq 0, \quad p_i \geq 0, \quad i = 1, \dots, N-1. \quad (32f)$$

However, it is challenging to directly calculate the partial derivative in (32a) due to the lack of the closed-form expressions for the achievable rate  $R_{F,i}(p_i)$ . Therefore, we aim to address this difficulty by exploiting the relationship between the mutual information and MMSE. Specifically, the MMSE of  $X_i$  is given as

$$\text{MMSE}_i(\text{SNR}_i) = \mathbb{E} \left\{ \left| X_i - \hat{X}_i \right|^2 \right\}, \quad (33)$$

where  $\text{SNR}_i = \frac{|H_i|^2 p_i}{\sigma^2 W}$  is the signal-to-noise ratio of the  $i$ th subcarrier, and  $\hat{X}_i$  is conditional expectation of  $X_i$ , i.e.,  $\hat{X}_i = \mathbb{E} \{ X_i | Y_i = H_i \sqrt{p_i} X_i + Z_i \}$ . According to *Theorem 1* in [21], the relationship between the mutual information (11a) and the MMSE (33) is given by

$$\frac{\partial}{\partial \text{SNR}_i} I_i(X_i; Y_i) = \text{MMSE}_i(\text{SNR}_i). \quad (34)$$

Combining (11b) and (34), partial derivative of function  $R_{F,i}(p_i)$  can be written as

$$\frac{\partial R_{F,i}(p_i)}{\partial p_i} = \frac{|H_i|^2}{\sigma^2 W} \text{MMSE}_i \left( \frac{|H_i|^2}{\sigma^2 W} p_i \right). \quad (35)$$

By substituting (35) into (32a), we have

$$\frac{|H_i|^2}{\sigma^2 W} \text{MMSE}_i \left( \frac{|H_i|^2}{\sigma^2 W} p_i \right) = \lambda_1 \mathbb{E}^2 \{|X_i|\} + \lambda_2. \quad (36)$$

Then, according to (36), the power allocation  $p_i$  can be

obtained as

$$p_i = \frac{\sigma^2 W}{|H_i|^2} \text{MMSE}_i^{-1} \left[ \frac{\sigma^2 W}{|H_i|^2} (\lambda_1 \mathbb{E}^2 \{|X_i|\} + \lambda_2) \right], \quad (37)$$

where  $\text{MMSE}_i^{-1}(\cdot)$  is the inverse function of  $\text{MMSE}_i(\cdot)$  with domain in  $[0, 1]$  and  $\text{MMSE}_i^{-1}(1) = 0$  [23]. Therefore, for the SE maximization problem (30), the optimal allocation power of the  $i$ th subcarrier is given by (38).

Meanwhile, according to the definition of MMSE,  $\lambda_1$  and  $\lambda_2$  should be greater than 0, otherwise the required power would be infinity. Therefore, substituting (38) into the complementary slackness conditions (32b) and (32c), the dual variables  $\lambda_1$  and  $\lambda_2$  is the solution of the following equation:

$$\sum_{i=1}^{N-1} \frac{\sigma^2 W}{|H_i|^2} \text{MMSE}_i^{-1} \left[ \frac{\sigma^2 W}{|H_i|^2} (\lambda_1 \mathbb{E}^2 \{|X_i|\} + \lambda_2) \right] \mathbb{E}^2 \{|X_i|\} = \frac{NP_o^2}{2(N-1)}, \quad (39a)$$

$$\sum_{i=1}^{N-1} \frac{\sigma^2 W}{|H_i|^2} \text{MMSE}_i^{-1} \left[ \frac{\sigma^2 W}{|H_i|^2} (\lambda_1 \mathbb{E}^2 \{|X_i|\} + \lambda_2) \right] = \frac{P_e}{4N-2}, \quad (39b)$$

which can be obtained by the multi-level mercury-water-filling power allocation scheme as listed in Algorithm 1 [22], [23]. Moreover, to facilitate the explanation of the power allocation scheme, an auxiliary function  $G_i(\lambda_1, \lambda_2)$  is defined as follows (40). Then, the allocated power  $p_i$  can be represented as

$$p_i = \frac{1}{\lambda_1 \mathbb{E}^2 \{|X_i|\} + \lambda_2} - \frac{|H_i|^2}{\sigma^2 W} G_i(\lambda_1, \lambda_2). \quad (41)$$

## V. ENERGY EFFICIENCY MAXIMIZATION OF THE DCO-OFDM SYSTEM

In this section, we propose the optimal power allocation schemes to maximize the EE of the DCO-OFDM system subject to the minimum SE threshold, the maximum average optical power and the maximum total electrical transmitted power constraints. We first investigate the EE maximization problem based on the lower bound  $R_{L,\text{total}}(\{p_i\})$  in (15) with the closed-form expression, and then study the case based on the exact achievable rate  $R_{F,\text{total}}(\{p_i\})$  in (12) without a closed-form expression.

---

### Algorithm 1 Multi-level Mercury-water-filling Power Allocation Scheme

---

**Input:** Given  $\lambda_1 \in [0, \hat{\lambda}_1]$ ,  $\delta_1 > 0$ , where  $\hat{\lambda}_1$  is the upper bound of  $\lambda_1$  and  $\delta_1$  is a small positive constant that controls the algorithm accuracy. Initialize  $\lambda_{\min} = 0$ ,  $\lambda_{\max} = \hat{\lambda}_1$ ;

- 1: **while**  $\lambda_{\max} - \lambda_{\min} \geq \delta_1$  **do**
- 2:   Set  $\lambda_1 = (\lambda_{\min} + \lambda_{\max})/2$ ;
- 3:   Find the minimum  $\lambda_2 \geq 0$ , with which 
$$\sum_{i=1}^{N-1} \left[ \frac{\sigma^2 W}{|H_i|^2} \text{MMSE}_i^{-1} \left[ \frac{\sigma^2 W}{|H_i|^2} (\lambda_1 \mathbb{E}^2 \{|X_i|\} + \lambda_2) \right] \right]^+ \leq \frac{P_e}{4N-2};$$
- 4:   If  $\lambda_1 \mathbb{E}^2 \{|X_i|\} + \lambda_2 \leq |H_i|^2 / \sigma^2 W$ , substitute  $\lambda_1, \lambda_2$  to obtain 
$$p_i^{\text{opt}} = \frac{\sigma^2 W}{|H_i|^2} \text{MMSE}_i^{-1} \left[ \frac{\sigma^2 W}{|H_i|^2} (\lambda_1 \mathbb{E}^2 \{|X_i|\} + \lambda_2) \right];$$
 otherwise  $p_i^{\text{opt}} = 0$ ;
- 5:   If  $\sum_{i=1}^{N-1} p_i^{\text{opt}} \mathbb{E}^2 \{|X_i|\} \leq \frac{NP_o^2}{2(N-1)}$ , set  $\lambda_{\max} \leftarrow \lambda_1$ ; otherwise  $\lambda_{\min} \leftarrow \lambda_1$ ;
- 6: **end while**

**Output:**  $p_i^{\text{opt}}$ ;

---

#### A. EE Maximization based on $R_{L,\text{total}}(\{p_i\})$

Based on the rate expression (15), the EE is given by

$$\text{EE}_L(\{p_i\}) = \frac{R_{L,\text{total}}(\{p_i\})}{2 \sum_{i=1}^{N-1} p_i + P_{\text{dc}} + P_c}, \quad (42)$$

where  $P_{\text{dc}} = \sum_{k=0}^{2N-1} \mathbb{E} \{(I_{\text{dc}})^2\}$  denotes the DC-bias power and  $P_c$  is the constant total circuit consumption of the whole system.

Therefore, the corresponding EE maximization problem can be formulated as

$$\underset{\{p_i\}, I_{\text{dc}}}{\text{maximize}} \quad \text{EE}_L(\{p_i\}) \quad (43a)$$

$$\text{s.t.} \quad (17b), (17c), (17d), (17e),$$

$$\text{SE}_L(\{p_i\}) \geq \gamma, \quad (43b)$$

where  $\gamma = \frac{\bar{R}}{2NW}$  is the minimum SE requirement of the DCO-OFDM system, and  $\bar{R}$  is the corresponding minimum threshold of the total achievable rate.

To ensure that there is no loss of information during the clipping operation, the value of  $I_{\text{dc}}$  is given in (20), and  $P_{\text{dc}}$

$$p_i^{\text{opt}} = \begin{cases} \frac{\sigma^2 W}{|H_i|^2} \text{MMSE}_i^{-1} \left[ \frac{\sigma^2 W}{|H_i|^2} (\lambda_1 \mathbb{E}^2 \{|X_i|\} + \lambda_2) \right], & 0 < \lambda_1 \mathbb{E}^2 \{|X_i|\} + \lambda_2 \leq \frac{|H_i|^2}{\sigma^2 W}, \\ 0, & \text{otherwise.} \end{cases} \quad (38)$$

$$G_i(\lambda_1, \lambda_2) \triangleq \begin{cases} \frac{|H_i|^2}{\sigma^2 W (\lambda_1 \mathbb{E}^2 \{|X_i|\} + \lambda_2)} - \text{MMSE}_i^{-1} \left[ \frac{\sigma^2 W}{|H_i|^2} (\lambda_1 \mathbb{E}^2 \{|X_i|\} + \lambda_2) \right], & 0 < \lambda_1 \mathbb{E}^2 \{|X_i|\} + \lambda_2 \leq \frac{\sigma^2 W}{|H_i|^2}; \\ 1, & \text{otherwise.} \end{cases} \quad (40)$$

is given as

$$P_{\text{dc}} = \sum_{k=0}^{2N-1} \mathbb{E} \left\{ \left( I_{\text{dc}}^{\text{non-clipping}} \right)^2 \right\} = 4\mathbb{E} \left\{ \left( \sum_{i=1}^{N-1} \sqrt{p_i} |X_i| \right)^2 \right\} \quad (44)$$

Thus, the original joint optimization problem (43) is converted into a concave-concave fractional problem, which is still complex and hard to solve. To overcome this challenge,  $P_{\text{dc}}$  in (44) is reformulated based on the Cauchy-Schwarz inequality (22) and is given by

$$P_{\text{dc}} \leq 4\mathbb{E} \left\{ (N-1) \sum_{i=1}^{N-1} p_i |X_i|^2 \right\} = 4(N-1) \sum_{i=1}^{N-1} p_i. \quad (45)$$

Based on (45), the denominator of (42) can be treated as an affine function of  $p_i$ . Thus, problem (43) can be transformed into a concave-linear fractional problem with variable  $p_i$ .

Similar to the SE maximization problem, the average optical power constraint (17c) and total electrical transmitted power constraint (17d) can be reformulated as (28b) and (28c), respectively. Therefore, the EE maximization problem (43) can be reformulated as

$$\underset{\{p_i\}}{\text{maximize}} \quad \frac{R_{\text{L,total}}(\{p_i\})}{(4N-2) \sum_{i=1}^{N-1} p_i + P_c} \quad (46a)$$

$$\text{s.t.} \quad (28b), (28c), (28d), \\ \text{SE}_{\text{L}}(\{p_i\}) \geq \gamma. \quad (46b)$$

Note that those constraints of problem (46) form a convex feasible solution set. It can be seen from the objective function (46a) that the numerator  $R_{\text{L,total}}(\{p_i\})$  is concave over its input power and the denominator is an affine function of  $p_i$ . In the following, we employ Dinkelbach-type iterative algorithm [40], [41] to handle this concave-linear fractional problem by converting problem (46) into a sequence of convex subproblems. In particular, by iteratively solving these convex subproblems, the globally optimal solution of problem (46) can be obtained eventually [42].

Let us define a new function  $f(\{p_i\}, q)$  as follow

$$f(\{p_i\}, q) \triangleq R_{\text{L,total}}(\{p_i\}) - q \left[ (4N-2) \sum_{i=1}^{N-1} p_i + P_c \right], \quad (47)$$

where  $q$  is a real parameter to be found iteratively. When  $q$  is as large as possible, the optimal solution of problem (46) can be obtained by calculating the roots of the equation  $f(\{p_i\}, q) = 0$  in the feasible constraint set [42].

For a given  $q$  in each iteration, the convex subproblem over  $p_i$  can be expressed as

$$\underset{\{p_i\}}{\text{maximize}} \quad f(\{p_i\}, q) \quad (48) \\ \text{s.t.} \quad (28b), (28c), (28d), (46b).$$

Since the optimization problem (48) has a concave objective function over its input power and linear constraints, the optimal

power  $p_i^{\text{opt}}$  of problem (48) can be obtained by the interior-point algorithm. Such as the barrier method, it transforms the convex optimization problems into a sequence of equality constrained problems and applies Newton's method to them, or such as the primal-dual interior-point method, it modifies the corresponding KKT conditions and solves them by Newton's method [37], [38]. Besides, It has been implemented by standard convex optimization solvers such as CVX [39].

Finally, the EE maximization problem for the lower bound of achievable rate can be solved by the Dinkelbach-type algorithm. The Dinkelbach-type algorithm is guaranteed to converge to the optimal solution of problem (46) with a finite number of iterations [40]–[42]. The details of implementation are shown in algorithm 2.

Similarly, the  $\text{EE}_{\text{A}}$  can be defined with  $R_{\text{L,total}}(\{p_i\})$ , and the corresponding EE maximization power allocation problem can be built and solved as similar to the problem (43).

---

#### Algorithm 2 Dinkelbach-type Power Allocation Scheme

---

**Input:** Given  $\delta \rightarrow 0, n = 0, p_i^{\text{opt}} > 0, q^{(n)} = 0$ ;  
1: **while**  $|q^{(n)} - q^{(n+1)}| \leq \delta$  **do**  
2:   Compute the optimal solution  $p_i^{\text{opt}}$  in (48);  
3:   Calculating the value of function  $f(\{p_i^{\text{opt}}\}, q^{(n)})$ ;  
4:    $q^{(n+1)} = \text{EE}_{\text{L}}(\{p_i^{\text{opt}}\})$ ;  
5:    $n = n + 1$ ;  
6: **end while**  
**Output:**  $\text{EE}_{\text{L}}(\{p_i^{\text{opt}}\})$ .

---

#### B. EE Maximization based on $R_{\text{F,total}}(\{p_i\})$

By applying the exact achievable rate expression given by (12), the EE of finite-alphabet inputs can be expressed as

$$\text{EE}_{\text{F}}(\{p_i\}) = \frac{R_{\text{F,total}}(\{p_i\})}{2 \sum_{i=1}^{N-1} p_i + P_{\text{dc}} + P_c}. \quad (49)$$

Then, the EE maximization problem with finite-alphabet inputs can be reformulated as

$$\underset{\{p_i\}}{\text{maximize}} \quad \text{EE}_{\text{F}}(\{p_i\}) \quad (50a)$$

$$\text{s.t.} \quad (28b), (28c), (28d), \\ \text{SE}_{\text{F}}(\{p_i\}) \geq \gamma. \quad (50b)$$

Here,  $P_{\text{dc}}$  in the denominator of (50a) takes the same value and constraint as (44) and (45). Due to the concave numerator  $R_{\text{F,total}}(\{p_i\})$  in (50a), problem (50) is also a concave-linear fractional problem, which can also be solved by Dinkelbach-type algorithms.

## VI. SIMULATION RESULTS AND DISCUSSION

In this section, we present numerical results to illustrate the proposed power allocation schemes for the SE and EE maximization problems of the DCO-OFDM VLC system. We consider the above DCO-OFDM VLC system is in a  $(5 \times 5 \times 3) \text{ m}^3$  room equipped with four LED lights, and the origin  $(0, 0, 0)$  of the three-dimensional Cartesian coordinate



system  $(X, Y, Z)$  is located at one corner on the floor of the square room. The receiver is located at  $(0.5, 1, 0)$ m, and the four LEDs are respectively located at  $(1.5, 1.5, 3)$ m,  $(1.5, 3.5, 3)$ m,  $(3.5, 1.5, 3)$ m, and  $(3.5, 3.5, 3)$ m. The other basic parameters of the system are listed in Table I.

TABLE I: Simulation Parameters of the DCO-OFDM VLC System.

Definition	Value
Half the number of subcarriers, $N$	16
Room size	$(5 \times 5 \times 3)$ m <sup>3</sup>
FOV, $\Psi$	90°
Lambertian emission order, $m$	1
Half power angle, $\Phi_{1/2}$	60°
PD collection area, $A_r$	1 cm <sup>2</sup>
Reflectivity factor, $\rho$	0.8
Circuit power consumption, $P_c$	0.1 W
Optical filter gain of receiver, $T(\varphi)$	0 dB
Concentrator gain of receiver, $G(\varphi)$	0 dB
Noise PSD, $\sigma^2$	$10^{-18}$ A <sup>2</sup> /Hz
Modulation scheme	4-QAM
Bandwidth of each subcarrier, $W$	1 MHz

TABLE II: The tightness of the original constraints (17b), (17c), (17d) and (17e) for the solution of problem (17).

Value / Definition	Scenarios	
	$P_o = 0.5$ W, $P_e = 20$ W	$P_o = 0.8$ W, $P_e = 10$ W
$I_{dc}^{\text{non-clipping}}$	0.4991	0.5491
$\min(x_k)$	-0.4052	-0.4175
$\mathbb{E}\{x_{dc,k}\}$	0.4991 W	0.5491 W
$\sum_{k=0}^{2N-1} \mathbb{E}\{x_{dc,k}^2\}$	8.2369 W	9.9698 W

In order to solve problem (17), we use inequality to deal with constraints (17b), (17c), (17d) and (17e) into (28b), (28c) and (28d). To verify the validity of the inequality treated constraints, we substitute the obtained solution of problem (28) into the original constraints (17b), (17c) and (17d). The tightness of the original constraints (17b), (17c), (17d) and (17e) for the solutions of problem (17) is shown in Table II. It can be seen that in the scenario of  $P_o = 0.5$  W and  $P_e = 20$  W,  $\mathbb{E}\{x_{dc,k}\} = 0.4991$  W, thus constraint (17c), i.e.,  $\mathbb{E}\{x_{dc,k}\} \leq P_o$ , is almost tight, while in the scenario of  $P_o = 0.8$  W and  $P_e = 10$  W,  $\sum_{k=0}^{2N-1} \mathbb{E}\{x_{dc,k}^2\} = 9.9698$  W, thus constraint (17d), i.e.,  $\sum_{k=0}^{2N-1} \mathbb{E}\{x_{dc,k}^2\} \leq P_e$ , is almost tight. Therefore, our treatment of constraints is valid and the obtained optimal solutions are also high-quality solutions for original problems.

#### A. Simulation Results of SE Maximization Problems

In this subsection, we present the results of the proposed power allocation schemes for maximizing the SE for finite-alphabet inputs and lower bound of the mutual information.

In order to illustrate the effect of the difference between channel gain of each subcarrier on power allocation, the

channel gain  $H_i$ , i.e., equation (9), of half subcarriers is shown in Fig. 2 (a). It can be seen from Fig. 2 (a) that the channel model in our DCO-OFDM system also has low-pass characteristics. As the subcarrier index  $i$  increases, the corresponding channel gain  $H_i$  decreases. The reason is that the channel gain  $H_i$  varies over the subcarrier in the dispersive channel model and high-frequency subcarriers correspond to higher subcarrier index  $i$ .

Fig. 2 (b) shows the achievable rate  $R_{F,i}$ , i.e., equation (11b), versus the allocated power  $p_i$ , in the case of  $i = 1$  and  $i = 15$ . It can be seen that as the allocated power  $p_i$  increases, the achievable rate  $R_{F,1}$  and  $R_{F,15}$  first increase fast and then increase slowly, and  $R_{F,1}$  gradually approaches  $\log_2 M$  ( $M = 4$ ). This is because the mutual information of  $M$ -ary discrete constellation modulation can not exceed  $\log_2 M$ . Moreover,  $R_{F,1}$  is higher than  $R_{F,15}$  since  $H_1 > H_{15}$ .

Fig. 2 (c) shows the gradient function  $\frac{\partial R_{F,i}}{\partial p_i}$ , i.e., equation (35), versus the allocated power  $p_i$ , in the case of  $i = 1$  and  $i = 15$ . It can be seen that both  $\frac{\partial R_{F,1}}{\partial p_1}$  and  $\frac{\partial R_{F,15}}{\partial p_{15}}$  decrease with the increase of  $p_i$ , and eventually tend to 0. When  $p_i \leq 5.134$  mW,  $\frac{\partial R_{F,1}}{\partial p_1} \geq \frac{\partial R_{F,15}}{\partial p_{15}}$ ; when  $p_i > 5.134$  mW,  $\frac{\partial R_{F,1}}{\partial p_1} < \frac{\partial R_{F,15}}{\partial p_{15}}$ . Fig. 2 (b) illustrates that, compared with subcarriers with small channel gains, when the allocated power is small, the subcarriers with large channel gains have larger gradient of rate. When the allocated power is large, the subcarriers with large channel gains have smaller gradient of rate.

In the following, three different power allocation scenarios for the SE maximization problem (30) are compared in the case of low, medium, and high total transmitted power. Specially, Fig. 3 (a), (b) and (c) are achieved with the same average optical power  $P_o = 10$  W, and different total electrical transmitted power  $P_e = 2$  W,  $P_e = 10$  W and  $P_e = 50$  W respectively.

It can be seen from Fig. 3 (a) that when the total allocated power is low ( $P_e = 2$  W), more power is allocated to subcarriers with larger channel gains, which is similar to the classical water-filling solution with the Gaussian distribution inputs. Combining Fig. 3 (a) and Fig. 2, it can be seen that this is because when the allocated power is small, the rate of the subcarriers with larger channel gains increases faster than the subcarriers with smaller channel gains, thus more power should be allocated to the subcarriers with larger gradient of rate to maximize the SE<sub>F</sub> of the system.

Fig. 3 (b) shows that for the case of medium total allocated power ( $P_e = 10$  W), more power is allocated to the subcarriers with moderate channel gains. Combining Fig. 3 (b) and Fig. 2, it can be seen that this is because as the allocated power increases, the rate of subcarriers with smaller channel gains increases faster than the rate of subcarriers with larger channel gains at this time. Therefore, more power is allocated to the subcarriers with smaller channel gains to maximize the SE<sub>F</sub> of the system, i.e., power is always preferentially allocated to the subcarrier with the largest gradient of rate.

It can be seen from Fig. 3 (c) that when the total allocated power is high ( $P_e = 50$  W), more power is allocated to subcarriers with smaller channel gains, which is exactly opposite with the water-filling policy. Combining Fig. 3 (c) and Fig. 2,

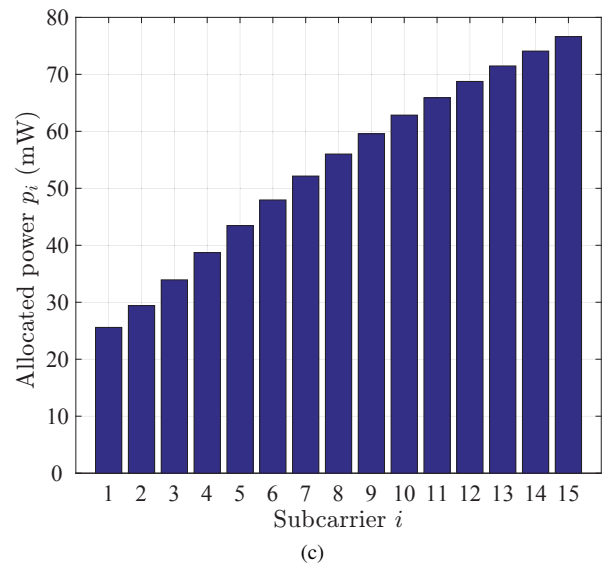
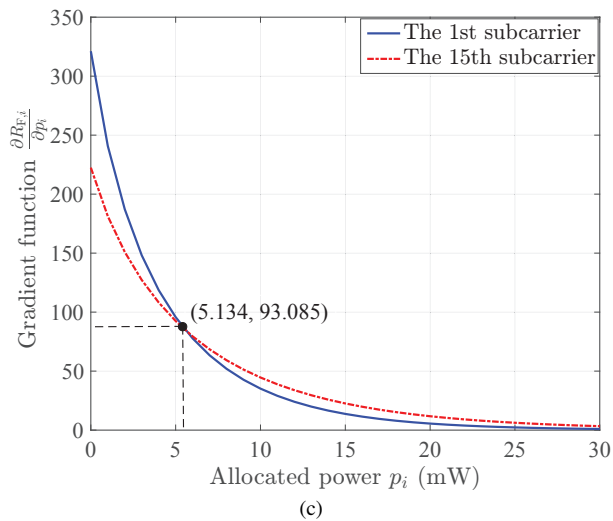
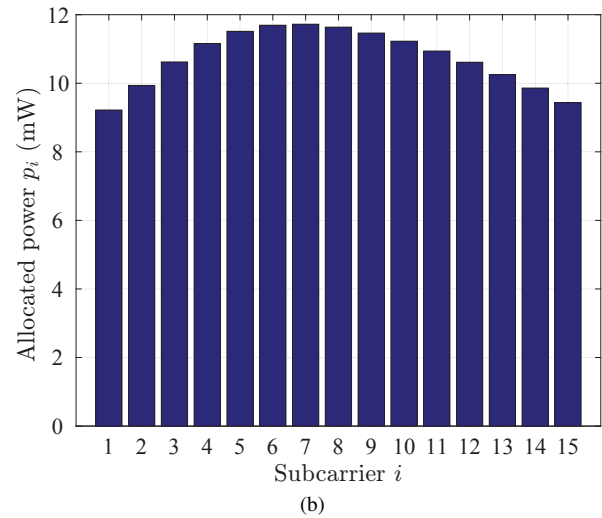
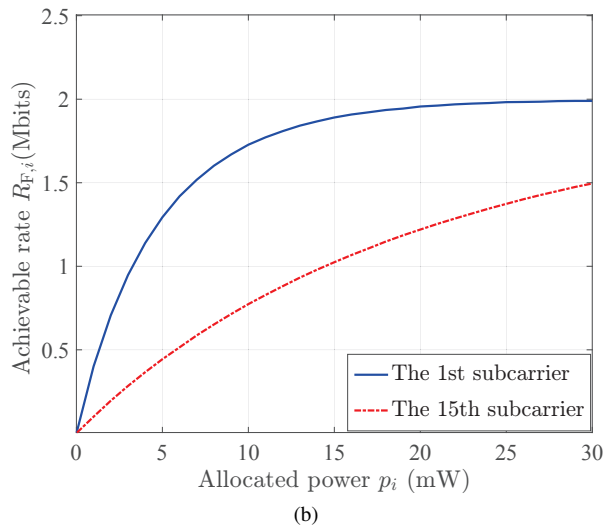
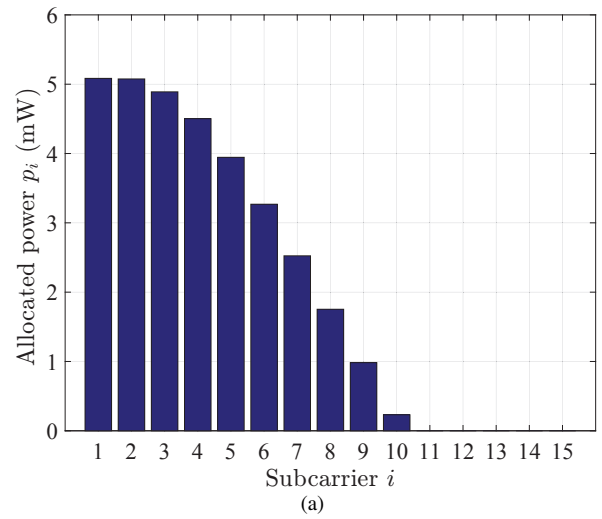
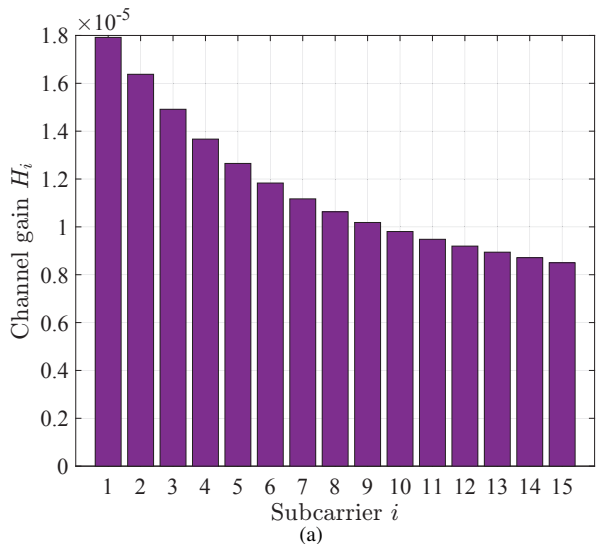


Fig. 2: (a) Channel gain  $H_i$  of subcarrier  $i$ ; (b) Achievable rate  $R_{F,i}$  versus the allocated power  $p_i$ ; (c) Gradient function  $\frac{\partial R_{F,i}}{\partial p_i}$  versus the allocated power  $p_i$ .

Fig. 3: Allocated power  $p_i$  of subcarrier  $i$  of SEF with  $P_o = 10$  W (a)  $P_e = 2$  W; (b)  $P_e = 10$  W; (c)  $P_e = 50$  W.

it can be seen that in this case, the rate of subcarriers with larger channel gains tends to be saturated ( $\log_2 M$ ), thus there is little incentive to allocate further power to such subcarriers. Rather, to maximize the  $SE_F$  of the system, the additional power is better allocated to subcarriers with smaller channel gains whose rate is still far from saturation.

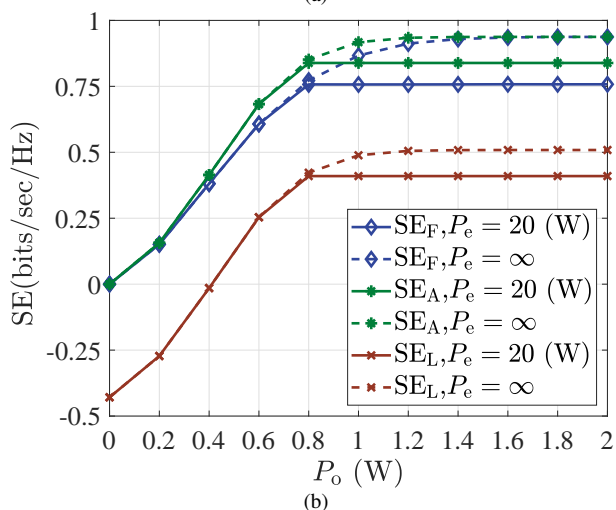
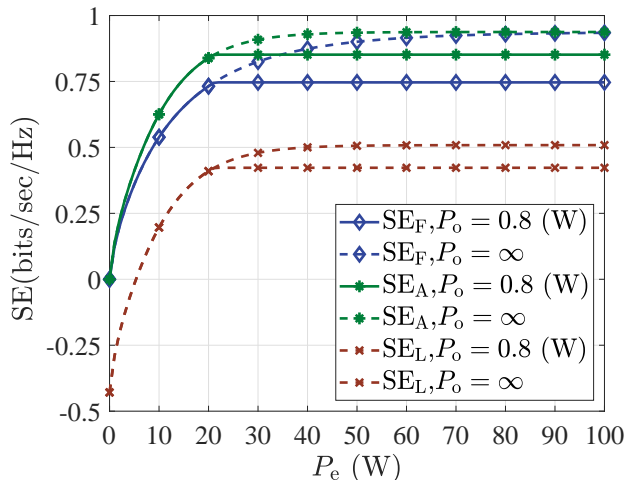


Fig. 4: (a)  $SE_F$ ,  $SE_A$  and  $SE_L$  versus electrical power budget  $P_e$  with two different optical power budget  $P_o = 0.8$  W and  $P_o = \infty$ ; (b)  $SE_F$ ,  $SE_A$  and  $SE_L$  versus optical power budget  $P_o$  with two different electrical power budget  $P_e = 20$  W and  $P_e = \infty$ .

Fig. 4 (a) illustrates  $SE_F$ ,  $SE_A$  and  $SE_L$  versus total electrical transmitted power budget  $P_e$  with two different optical power budget  $P_o = 0.8$  W and  $P_o = \infty$  (without optical power constraint), respectively. For the case of  $P_o = 0.8$  W, as  $P_e$  increases,  $SE_F$ ,  $SE_A$  and  $SE_L$  first increase and then get restricted into a constant. The reason is that the total allocated power is restricted by the optical power  $P_o = 0.8$  W. For the case of  $P_o = \infty$ , as  $P_e$  increases,  $SE_F$ ,  $SE_A$  and  $SE_L$  first increase and then remain constant. This is because the mutual information of  $M$ -ary discrete constellation modulation can not exceed  $\log_2 M$ . Moreover, similar to  $SE_A$  and  $SE_L$ , when  $P_e > 20$  W,  $SE_F$  with  $P_o = \infty$  is higher than  $SE_F$  with  $P_o = 0.8$  W. This is because the total allocated power is restricted when  $P_o$  takes the value of 0.8 W. It can be seen that, using the optimal power allocation policy

proposed in this paper,  $SE_F$  is significantly higher than  $SE_L$  since  $R_{L,\text{total}}(\{p_i\})$  is the lower bound of  $R_{F,\text{total}}(\{p_i\})$ . Meanwhile,  $SE_F$  is slightly lower than  $SE_A$  in the medium  $P_e$ , however, they will tend to coincide when  $P_e \rightarrow \infty$  and  $P_e \rightarrow 0$ , which consistent with the feature of  $R_{A,\text{total}}(\{p_i\})$  [36].

Fig. 4 (b) depicts  $SE_F$ ,  $SE_A$  and  $SE_L$  versus average optical power budget  $P_o$  with two different electrical power budgets  $P_e = 20$  W and  $P_e = \infty$  (without electrical power constraint), respectively. For the case of  $P_e = 20$  W, as  $P_o$  increases,  $SE_F$ ,  $SE_A$  and  $SE_L$  first increase and then get restricted as a constant. This is because the total allocated power is limited by the electrical power budget  $P_e = 20$  W. When  $P_e = \infty$ , as  $P_o$  increases,  $SE_F$ ,  $SE_A$  and  $SE_L$  first increase and then remain constant. In addition, similar to  $SE_A$  and  $SE_L$ , when  $P_o > 0.6$  W,  $SE_F$  with  $P_e = \infty$  is higher than  $SE_F$  with  $P_e = 20$  W. This is because the total allocated power is restricted when  $P_e$  takes the value of 20 W. Besides, we can observe that  $SE_F$  is significantly higher than  $SE_L$ , and  $SE_A$  is slightly higher than  $SE_A$  but converges if  $P_e \rightarrow \infty$  and  $P_e \rightarrow 0$ .

### B. Simulation Results of EE Maximization Problems

In this subsection, we present the simulation results of the proposed power allocation schemes for maximizing the EE for finite-alphabet inputs and lower bound of the mutual information.

To illustrate the three scenarios when the SE threshold  $\gamma$  is small, medium and large, the allocated power  $p_i$  of subcarrier  $i$  of  $EE_F$  with  $\gamma = 0.156$  Mbits/sec/Hz ( $\bar{R} = 5$  Mbits/sec),  $\gamma = 0.469$  Mbits/sec/Hz ( $\bar{R} = 15$  Mbits/sec) and  $\gamma = 0.781$  Mbits/sec/Hz ( $\bar{R} = 25$  Mbits/sec), where  $P_o = 1$  W,  $P_e = 22$  W, are shown in Fig. 5 (a), (b) and (c) respectively.

It can be seen from Fig. 5 (a) that when the SE threshold  $\gamma$  is small ( $\gamma = 0.156$  Mbits/sec/Hz), more power is allocated to subcarriers with larger channel gains, and the required power increases with the improvement of the SE threshold  $\gamma$ . Besides, Fig. 2 (c) shows that the gradient of the rate increases synchronously with the channel gain. Thus, more power would be allocated to the subcarriers with a larger gradient of the rate to maximize the  $EE_F$  of the system.

Fig. 5 (b) shows that for the case of medium SE threshold  $\gamma$  ( $\gamma = 0.469$  Mbits/sec/Hz), more power is allocated to the subcarriers with moderate channel gains, and as the SE threshold  $\gamma$  increases, the power that needs to be allocated becomes larger. Combining with Fig. 2 (c), it can be seen that to maximize the  $EE_F$  of the system, the power is always preferentially allocated to the subcarrier with the largest gradient of the rate.

It can be seen from Fig. 5 (c) that when the SE threshold  $\gamma$  is large ( $\gamma = 0.781$  Mbits/sec/Hz), more power is allocated to subcarriers with smaller channel gains. Combining Fig. 5 (c) and Fig. 2 (c), it can be seen that when the allocated power  $p_i$  is large, to achieve the same gradient of the rate, the power allocated to subcarriers with larger channel gains is much greater than the power allocated to subcarriers with smaller channel gains. Thus, the additional power is preferentially allocated to subcarriers with smaller channel gains to maximize the  $EE_F$  of the system.

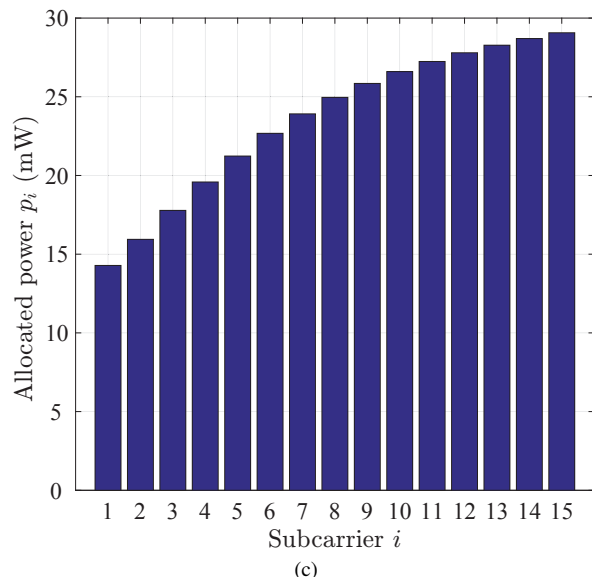
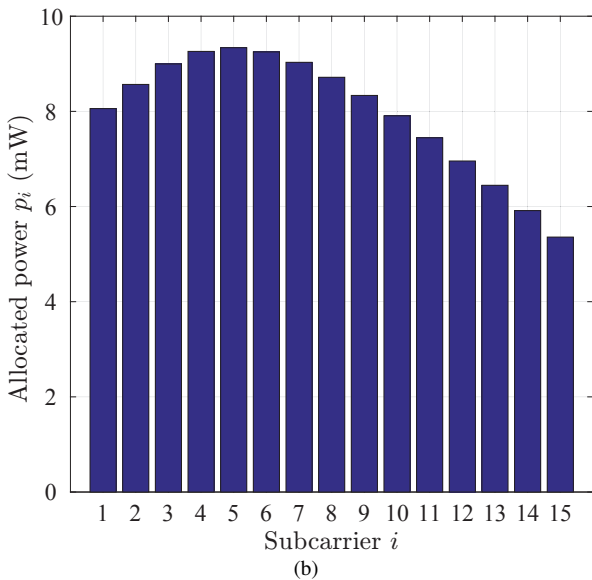
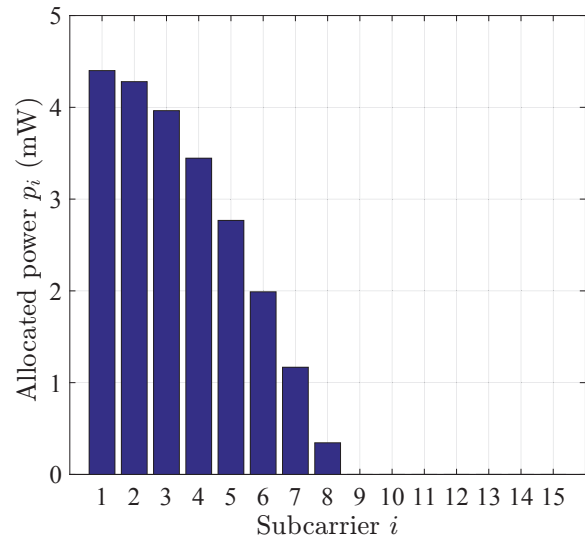


Fig. 5: Allocated power  $p_i$  of subcarrier  $i$  of  $EE_F$  with  $P_o = 1$  W,  $P_e = 22$  W, (a)  $\gamma = 0.156$  Mbits/sec/Hz ( $\bar{R} = 5$  Mbits/sec); (b)  $\gamma = 0.469$  Mbits/sec/Hz ( $\bar{R} = 15$  Mbits/sec); (c)  $\gamma = 0.781$  Mbits/sec/Hz ( $\bar{R} = 25$  Mbits/sec).

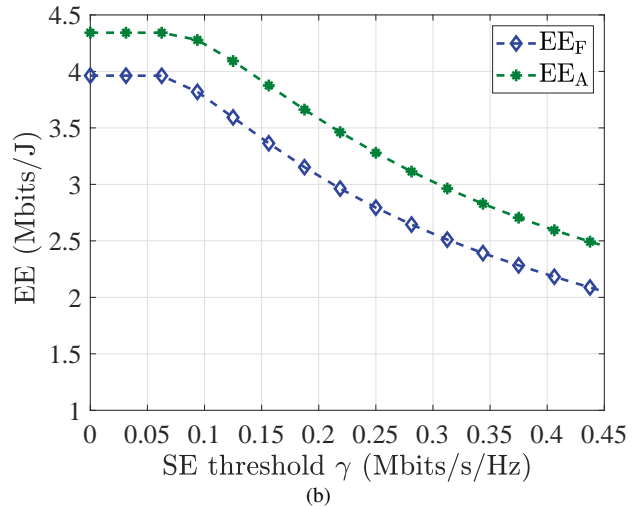
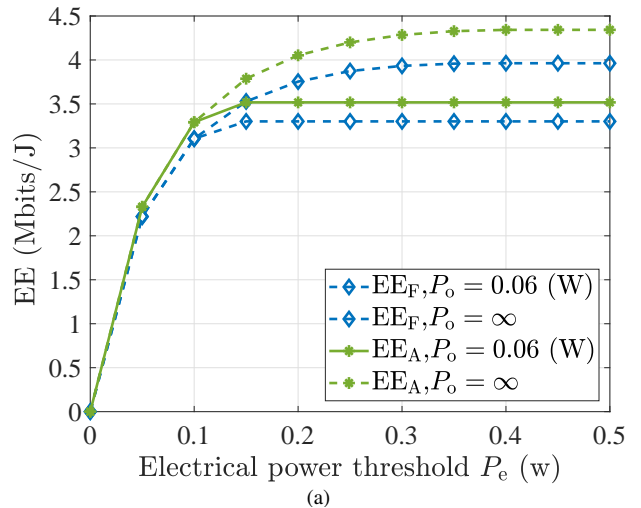


Fig. 6: (a)  $EE_F$  and  $EE_A$  versus electrical power budget  $P_e$  with SE threshold  $\gamma = 0.009$  Mbits/sec/Hz ( $\bar{R} = 0.3$  Mbits/sec) and two different optical power budget  $P_o = 0.06$  W and  $P_o = \infty$ ; (b)  $EE_F$ ,  $EE_A$  and  $EE_L$  versus SE threshold  $\gamma$  with electrical power budget  $P_e = 5$  W and optical power budget  $P_o = 1$  W.

Fig. 6 (a) illustrates  $EE_F$  and  $EE_A$  versus electrical power budget  $P_e$  with SE constraint  $\gamma = 0.009$  Mbits/sec/Hz ( $\bar{R} = 0.3$  Mbits/sec) and two different optical power budget  $P_o = 0.06$  W and  $P_o = \infty$  (without optical power constraint), respectively. For the case of  $P_o = 0.06$  W, as  $P_e$  increases,  $EE_F$  and  $EE_A$  first increase and then get restricted into a constant. The reason is that the total allocated power is restricted by the optical power  $P_o = 0.06$  W. For the case of  $P_o = \infty$ , as  $P_e$  increases,  $EE_F$  and  $EE_A$  first increase and then remain constant. This is because  $EE_F$  and  $EE_A$  remain constant when they reach their maximum values respectively. Moreover, similar to  $EE_A$ , for the large  $P_e$ ,  $EE_F$  with  $P_o = \infty$  is higher than  $EE_L$  with  $P_o = 0.06$  W since  $EE_L$  and  $EE_F$  are restricted when  $P_o$  takes the value of 0.06 W. It can be seen that  $EE_F$  is lower than  $EE_A$ .

Fig. 6 (b) depicts  $EE_F$  and  $EE_A$  versus SE threshold  $\gamma$  with electrical power budget  $P_e = 5$  W and optical power budget  $P_o = 1$  W. We observe that  $EE_F$  and  $EE_A$  both first keep stable and then decrease as SE threshold  $\gamma$  increases. This is because when the SE threshold  $\gamma$  is small, the performed

power allocation can easily satisfy the SE requirement and thus EE keeps as a constant. When the SE threshold  $\gamma$  becomes larger, more power needs to be consumed to satisfy the rate constraint, therefore the EE decreases.

### C. Simulation Results of Computational Complexity

In this subsection, we present the average executing time versus half of subcarrier number  $N$  to evaluate the computational complexity of the proposed power allocation schemes for SE- and EE-maximization problem. For given  $N$  and other fixed parameters, the average executing time is calculated according on 10000 repeated simulations, which are performed by MATLAB (2020b) with Intel(R) Core(TM) i9-10900K 3.70 GHz CPU and 32 GB RAM.

TABLE III: The average executing time (ms) of different scheme versus half of subcarrier number  $N$ .

Time \ Scheme	SE <sub>F</sub>	SE <sub>A</sub>	EE <sub>F</sub>	EE <sub>A</sub>
$N=4$	8.34	2.91	18220	1030
$N=8$	48.77	2.83	27630	1040
$N=16$	126.51	2.99	72500	1040

For the SE-maximization problem, through the mercury-water-filling method, Table III depicts the comparing of the scheme base on  $R_{F,\text{total}}(\{p_i\})$  and based on  $R_{A,\text{total}}(\{p_i\})$  with electrical power budget  $P_e = 20$  W and optical power budget  $P_o = 5$  W. As shows, the CPU time of the proposed schemes based on  $R_{F,\text{total}}(\{p_i\})$  increases as  $N$  increases, however, for the proposed schemes based on  $R_{A,\text{total}}(\{p_i\})$ , it almost is a constant. Meanwhile, it is obvious that the scheme based on  $R_{A,\text{total}}(\{p_i\})$  is much faster than the scheme based on  $R_{F,\text{total}}(\{p_i\})$ .

For the EE-maximization problem, Table III presents the difference of the scheme based on  $R_{F,\text{total}}(\{p_i\})$  and  $R_{A,\text{total}}(\{p_i\})$  with electrical power budget  $P_e = 20$  W, optical power budget  $P_o = 5$  W, and SE threshold  $\gamma = 0.009$  Mbits/sec/Hz, and we can draw a conclusion as same as the comparing between SE<sub>F</sub> and SE<sub>L</sub>.

## VII. CONCLUSION

In this work, we investigated the bound of the information transmission rate of the DCO-OFDM system with finite-alphabet inputs, and proposed the optimal power allocation schemes to achieve maximum SE and maximum EE of the DCO-OFDM system, respectively. We first derived the exact achievable rate expression without information loss. Then, we developed the power allocation to maximize SE based on the lower bound of achievable rate. Furthermore, we exploited the KKT conditions and the relationship between the mutual information and MMSE, and derived the multi-level mercury-water-filling power allocation scheme for SE maximization. Moreover, we proposed the Dinkelbach-type power allocation scheme and obtained the optimal power allocation for EE maximization. Finally, numerical results revealed that the proposed multi-level mercury-water-filling scheme of SE maximization based on the exact mutual information depends on both channel gain of each subcarrier and the total

transmitted power constraint. When the total transmitted power is high, the power allocation of each subcarrier is inversely proportional to the channel gain, which is different from that of the classical water-filling method. Besides, we revealed that for the EE maximization problem with finite-alphabet inputs, the power allocation of each subcarrier is proportional to the channel gain for the low SE requirement. While for the high SE requirement, the power allocation of each subcarrier is inversely proportional to the channel gain. Besides, under the same constraints, the value of SE and EE based on the exact mutual information is always higher than that based on the lower bound.

## APPENDIX A PROOF OF (11b)

According to equation (10), the conditional probability density function  $p(Y_i|X_i)$  and the probability density function  $p(Y_i)$  corresponding to the channel output  $Y_i$  are respectively expressed as

$$p(Y_i|X_i) = \frac{1}{\pi\sigma^2W} \exp\left(-\frac{|Y_i - H_i\sqrt{p_i}X_i|^2}{\sigma^2W}\right), \quad (51a)$$

$$p(Y_i) = \mathbb{E}_{X_i} \{p(Y_i|X_i)\} = \frac{1}{M} \sum_{k=1}^M p(Y_i|X_{i,k}). \quad (51b)$$

Then, the mutual information between the channel input  $X_i$  and channel output  $Y_i$  can be obtained as

$$I(X_i; Y_i) = W \sum_{X_i} \int_{Y_i} p(X_i, Y_i) \log_2 \frac{p(X_i, Y_i)}{p(X_i)p(Y_i)} dY_i \quad (52a)$$

$$= W \sum_{n=1}^M \int_{Y_i} \frac{1}{M} p(Y_i|X_{i,n}) \log_2 \frac{p(Y_i|X_{i,n})}{p(Y_i)} dY_i \quad (52b)$$

$$= \frac{W}{M} \sum_{n=1}^M \int_{Y_i} p(Y_i|X_{i,n}) \log_2 \frac{p(Y_i|X_{i,n})}{\sum_{k=1}^M \frac{1}{M} p(Y_i|X_{i,k})} dY_i \quad (52c)$$

$$= \frac{W}{M} \sum_{n=1}^M \int_{Y_i} p(Y_i|X_{i,n}) \log_2 \frac{\exp\left(-\frac{|Y_i - H_i\sqrt{p_i}X_{i,n}|^2}{\sigma^2W}\right)}{\sum_{k=1}^M \frac{1}{M} \exp\left(-\frac{|Y_i - H_i\sqrt{p_i}X_{i,k}|^2}{\sigma^2W}\right)} dY_i \quad (52d)$$

$$= -\frac{W}{M} \sum_{n=1}^M \int_{Z_i} p(Z_i) \log_2 \sum_{k=1}^M \frac{1}{M} \exp\left(-d_{n,k} + \frac{|Z_i|^2}{\sigma^2W}\right) dZ_i \quad (52e)$$

$$= -\frac{W}{M} \sum_{n=1}^M \mathbb{E}_{Z_i} \left\{ \log_2 \sum_{k=1}^M \frac{1}{M} \exp\left(-d_{n,k} + \frac{|Z_i|^2}{\sigma^2W}\right) \right\} \quad (52f)$$

$$= -\frac{W}{M} \sum_{n=1}^M \mathbb{E}_{Z_i} \left\{ \log_2 \frac{1}{M} \exp\left(\frac{|Z_i|^2}{\sigma^2W}\right) \right\} - \frac{W}{M} \sum_{n=1}^M \mathbb{E}_{Z_i} \left\{ \log_2 \sum_{k=1}^M \exp(-d_{n,k}) \right\} \quad (52g)$$

$$\begin{aligned}
&= -\frac{W}{M} \sum_{n=1}^M \mathbb{E}_{Z_i} \left\{ \log_2 \left( \frac{\exp\left(\frac{|Z_i|^2}{\sigma^2 W}\right) \sum_{k=1}^M \exp(-d_{n,k})}{M} \right) \right\} \\
&= W \left( \log_2 M - \frac{1}{\ln 2} \right) \\
&\quad - \sum_{n=1}^M \frac{W}{M} \mathbb{E}_{Z_i} \left\{ \log_2 \sum_{k=1}^M \exp(-d_{n,k}) \right\}, \quad (52i)
\end{aligned}$$

where (52c) is due to (51b), (52d) is due to (51a),  $d_{n,k} \triangleq \frac{|H_i \sqrt{p_i}(X_{i,n} - X_{i,k}) + Z_i|^2}{\sigma^2 W}$  and the first term in (52i) is based on  $\mathbb{E}_{Z_i} \left\{ |Z_i|^2 \right\} = \sigma^2 W$ .

## REFERENCES

- [1] M. A. Razzaque, M. Milojevic-Jevric, A. Palade, and S. Clarke, "Middleware for internet of things: A survey," *IEEE Internet Things J.*, vol. 3, no. 1, pp. 70–95, Nov. 2016.
- [2] A. Zanella, N. Bui, A. Castellani, L. Vangelista, and M. Zorzi, "Internet of things for smart cities," *IEEE Internet Things J.*, vol. 1, no. 1, pp. 22–32, Feb. 2014.
- [3] V. W. S. Wong, R. Schober, D. W. K. Ng, and L. Wang, Eds., *Key Technologies for 5G Wireless Systems*, Cambridge, U.K.: Cambridge Univ. Press, Apr. 2017.
- [4] L. Feng, H. Yang, R. Q. Hu, and J. Wang, "MmWave and VLC-based indoor channel models in 5G wireless networks," *IEEE Wireless Commun.*, vol. 25, no. 5, pp. 70–77, Oct. 2018.
- [5] P. D. Diamantoulakis, G. K. Karagiannidis, and Z. Ding, "Simultaneous lightwave information and power transfer (SLIPT)," *IEEE Trans. Green Commun. Netw.*, vol. 2, no. 3, pp. 764–773, Sep. 2018.
- [6] *IEEE standard for local and metropolitan area networks-part 15.7: short-range wireless optical communication using visible light*, IEEE Std 802.15.7-2011, Sep. 2011.
- [7] H. Haas, L. Yin, Y. Wang, and C. Chen, "What is LiFi?" *J. Lightw. Technol.*, vol. 34, no. 6, pp. 1533–1544, Dec. 2016.
- [8] X. Liu, Y. Wang, F. Zhou, S. Ma, R. Q. Hu, and D. W. K. Ng, "Beamforming design for secure MISO visible light communication networks with SLIPT," *IEEE Trans. Commun.*, vol. 68, no. 12, pp. 7795–7809, Dec. 2020.
- [9] A. Jovicic, J. Li, and T. Richardson, "Visible light communication: Opportunities, challenges and the path to market," *IEEE Commun. Mag.*, vol. 51, no. 12, pp. 26–32, Dec. 2013.
- [10] R. Zhang, J. Wang, Z. Wang, Z. Xu, C. Zhao, and L. Hanzo, "Visible light communications in heterogeneous networks: paving the way for user-centric design," *IEEE Wireless Commun.*, vol. 22, no. 2, pp. 8–16, Apr. 2015.
- [11] P. H. Pathak, X. Feng, P. Hu, and P. Mohapatra, "Visible light communication, networking, and sensing: A survey, potential and challenges," *IEEE Commun. Surveys Tuts.*, vol. 17, no. 4, pp. 2047–2077, 4th Quart. 2015.
- [12] H. Elgala, R. Mesleh, and H. Haas, "Indoor optical wireless communication: Potential and state-of-the-art," *IEEE Commun. Mag.*, vol. 49, no. 9, pp. 56–62, Sep. 2011.
- [13] H. Le Minh, D. O'Brien, G. Faulkner, L. Zeng, K. Lee, D. Jung, and Y. Oh, "High-speed visible light communications using multiple-resonant equalization," *IEEE Photon. Technol. Lett.*, vol. 20, no. 14, pp. 1243–1245, Jul. 2008.
- [14] A. T. Hussein and J. M. H. Elmoghani, "Mobile multi-gigabit visible light communication system in realistic indoor environment," *J. Lightw. Technol.*, vol. 33, no. 15, pp. 3293–3307, Jun. 2015.
- [15] S. Dimitrov and H. Haas, "Information rate of OFDM-based optical wireless communication systems with nonlinear distortion," *J. Lightw. Technol.*, vol. 31, no. 6, pp. 918–929, Mar. 2013.
- [16] L. Wu, Z. Zhang, J. Dang, and H. Liu, "Adaptive modulation schemes for visible light communications," *J. Lightw. Technol.*, vol. 33, no. 1, pp. 117–125, Jan. 2015.
- [17] X. Deng, S. Mardankorani, G. Zhou, and J. M. G. Linnartz, "DC-bias for optical OFDM in visible light communications," *IEEE Access*, vol. 7, pp. 98319–98330, Jul. 2019.
- [18] X. Ling, J. Wang, X. Liang, Z. Ding, and C. Zhao, "Offset and power optimization for DCO-OFDM in visible light communication systems," *IEEE Trans. Signal Process.*, vol. 64, no. 2, pp. 349–363, Jan. 2016.
- [19] X. Ling, J. Wang, X. Liang, Z. Ding, C. Zhao, and X. Gao, "Biased multi-LED beamforming for multicarrier visible light communications," *IEEE J. Sel. Areas Commun.*, vol. 36, no. 1, pp. 106–120, Jan. 2018.
- [20] J. Armstrong and B. J. C. Schmidt, "Comparison of asymmetrically clipped optical OFDM and DC-biased optical OFDM in AWGN," *IEEE Commun. Lett.*, vol. 12, no. 5, pp. 343–345, May 2008.
- [21] D. Guo, S. Shamai(Shitz), and S. Verdú, "Mutual information and minimum mean-square error in Gaussian channels," *IEEE Trans. Inf. Theory*, vol. 51, no. 4, pp. 1261–1282, Apr. 2005.
- [22] R. Zhang and Y.-C. Liang, "Exploiting multi-antennas for opportunistic spectrum sharing in cognitive radio networks," *IEEE J. Sel. Topics Signal Process.*, vol. 2, no. 1, pp. 88–102, 2008.
- [23] A. Lozano, A. M. Tulino, and S. Verdú, "Optimum power allocation for parallel Gaussian channels with arbitrary input distributions," *IEEE Trans. Inf. Theory*, vol. 52, no. 7, pp. 3033–3051, Jul. 2006.
- [24] S. Mardankorani, X. Deng, and J. M. G. Linnartz, "Sub-carrier loading strategies for DCO-OFDM LED communication," *IEEE Trans. Commun.*, vol. 68, no. 2, pp. 1101–1117, Feb. 2020.
- [25] J. Zhou and W. Zhang, "A comparative study of unipolar OFDM schemes in Gaussian optical intensity channel," *IEEE Trans. Commun.*, vol. 66, no. 4, pp. 1549–1564, Apr. 2018.
- [26] M. Kashef, M. Ismail, M. Abdallah, K. A. Qaraqe, and E. Serpedin, "Energy efficient resource allocation for mixed RF/VLC heterogeneous wireless networks," *IEEE J. Sel. Areas Commun.*, vol. 34, no. 4, pp. 883–893, Mar. 2016.
- [27] W. Guo, H. Zhang, and C. Huang, "Energy efficiency of two-way communications under various duplex modes," *IEEE Internet Things J.*, vol. 8, no. 3, pp. 1921–1933, Feb. 2021.
- [28] C. Xiong, G. Y. Li, S. Zhang, Y. Chen, and S. Xu, "Energy-and spectral-efficiency tradeoff in downlink OFDMA networks," *IEEE Trans. Wireless Commun.*, vol. 10, no. 11, pp. 3874–3886, Dec. 2011.
- [29] A. Weiss, A. Yeredor, and M. Shtaf, "Iterative symbol recovery for power-efficient DC-biased optical OFDM systems," *J. Lightw. Technol.*, vol. 34, no. 9, pp. 2331–2338, May 2016.
- [30] Y. Hei, Y. Kou, G. Shi, W. Li, and H. Gu, "Energy-spectral efficiency tradeoff in DCO-OFDM visible light communication system," *IEEE Trans. Veh. Technol.*, vol. 68, no. 10, pp. 9872–9882, Oct. 2019.
- [31] C. Xiao, Y. R. Zheng, and Z. Ding, "Globally optimal linear precoders for finite alphabet signals over complex vector Gaussian channels," *IEEE Trans. Signal Process.*, vol. 59, no. 7, pp. 3301–3314, Jul. 2011.
- [32] P. Ge, X. Liang, J. Wang, and C. Zhao, "Modulation order selection and power allocation for energy efficient VLC-OFDM systems," in *2017 9th International Conference on Wireless Communications and Signal Processing (WCSP)*, pp. 1–6, Oct. 2017.
- [33] J. M. Kahn and J. R. Barry, "Wireless infrared communications," *Proceedings of the IEEE*, vol. 85, no. 2, pp. 265–298, Feb. 1997.
- [34] H. Schulze, "Frequency-domain simulation of the indoor wireless optical communication channel," *IEEE Trans. Commun.*, vol. 64, no. 6, pp. 2551–2562, Jun. 2016.
- [35] R. Rajashekar, M. Di Renzo, L. Yang, K. V. S. Hari, and L. Hanzo, "A finite input alphabet perspective on the rate-energy tradeoff in SWIPT over parallel Gaussian channels," *IEEE J. Sel. Areas Commun.*, vol. 37, no. 1, pp. 48–60, Jan. 2019.
- [36] W. Zeng, C. Xiao, and J. Lu, "A low-complexity design of linear precoding for MIMO channels with finite-alphabet inputs," *IEEE Wireless Commun. Lett.*, vol. 1, no. 1, pp. 38–41, Feb. 2012.
- [37] S. Boyd and L. Vandenberghe, *Convex Optimization*, Cambridge, U.K.: Cambridge Univ. Press, 2004.
- [38] Joseph-Frédéric Bonnans, Jean Charles Gilbert, Claude Lemarechal, and Claudia A. Sagastizábal, *Numerical Optimization: Theoretical and Practical Aspects*, Universitext. Springer, Berlin ; New York, 2nd ed edition, 2006.
- [39] M. Grant and S. Boyd, "CVX: Matlab software for disciplined convex programming, version 2.1," <http://cvxr.com/cvx>, Mar. 2014.
- [40] W. Dinkelbach, "On nonlinear fractional programming," *Manage. Sci.*, vol. 13, no. 7, pp. 492–498, Mar. 1967.
- [41] J. P. G. Crouzeix and J. A. Ferland, "Algorithms for generalized fractional programming," *Math. Program.*, vol. 52, pp. 191–207, May 1991.
- [42] A. Zappone and E. Jorswieck, "Energy efficiency in wireless networks via fractional programming theory," *Found. Trends Commun. Inf. Theory*, vol. 11, no. 3-4, pp. 185–396, Jun. 2015.